On the Interplay between Advection and Diffusion in Closed Laminar Chaotic Flows

A. Adrover, S. Cerbelli, and M. Giona*

Dipartimento di Ingegneria Chimica Universitá di Roma "La Sapienza", via Eudossiana 18, 00184 Roma, Italy

Received: November 27, 2000

This article illustrates a new and simple approach to the analysis of the effects of diffusion in laminar chaotic flows. The approach is based upon the definition of two quantities, namely diffusional thickness and area of diffusional influence, which provide a compact and quantitative description of the spatiotemporal evolution of partially mixed structures. Several implications follow from this approach: (A) Dispersion in closed chaotic flows displays nonmonotonic behavior induced by the shrinking of diffusional thickness along the stable directions. A theoretical explanation of this phenomenon is provided. (B) It is possible to define a characteristic time corresponding to the blow-up of the geometric interface induced by the diffusional merging of lamellae. The implications of these results as regards the dynamics of other physicochemical processes such as chemical reactions are briefly addressed.

1. Introduction

Fluid mixing is a complex phenomenon that controls a variety of physicochemical processes involving fluid phases such as chemical reactions, aggregation phenomena, polymerization, crystallization, etc.[1−4] The two basic cooperative mechanisms are stirring (advection), i.e., the action of a forced velocity field, and diffusion, which can be molecular and/or turbulent.

Usually (though not invariably), turbulent flow conditions ensure the fast blending of fluid elements, and rate-limiting resistances to overall transport of solution components are to be found in other phenomena that occur along with the mixing process (e.g., coalescence and breakup, chemical kinetics, and so on). Conversely, transport in laminar flows is often dominated by mixing. An industrially relevant example is provided by reacting melts of highly viscous polymers, possibly characterized by complex rheological behavior, whose molecular weight distribution can depend heavily on the conditions of mechanical agitation during the reaction time.[6]

Beyond its practical importance, the realm of laminar flows also provides a simplified phenomenological framework for understanding the essence of a mixing process, i.e., the interplay between fluid mechanics (in the sense of advection), which controls the increase of material interfaces and the formation of spatially coherent structures, and diffusive transport, which smoothens the concentration profiles and interfacial discontinuities at shorter length scales.

If molecular diffusion is negligible, laminar mixing can be very conveniently approached in a Lagrangian way, by considering the kinematics of a fluid particle[5]:

$$\frac{d\mathbf{x}}{dt} = \mathbf{v}(\mathbf{x}, t) \tag{1}$$

where $\mathbf{x}(t)$ is particle position at time t and $\mathbf{v}$ the velocity field. Formally, the analysis of mixing is thus translated into a problem of dynamical system theory originated by the ordinary differential eq 1. In a diffusionless setting, the efficient mixing of two or more segregated species results in a complex intertwined lamellar structure with different species organized in an alternate array of striations. As time goes by, the interface between neighboring striations is stretched and folded toward a nested convoluted surface (a curve in two dimensions) that fills most of the mixing space densely, albeit with a high degree of nonuniformity. The overall growth rate of the interface is exponential in time.

Recent works focusing on the evolution of interfaces in laminar chaotic flows[7−9] have proved that, after a transient, the geometric features of the interface structure settle into a *stationary* behavior regardless of the initial (i.e., premixed) condition. The geometric template that governs chaotic advection thus depends uniquely upon the mixing protocol.

When diffusion is accounted for, the physical framing of mixing is a more delicate problem. The current literature on laminar chaotic flows with diffusion addresses this issue primarily in statistical terms by focusing on the scaling of the mean square displacement of a fluid particle advected by the flow and subjected to random fluctuations in its motion.[10−13] This is the classical approach to dispersion based on Monte Carlo simulations, which rests on the equivalence between diffusion and uncorrelated random processes.

The other classical (Eulerian) approach is based on the solution of the corresponding advection/diffusion/(reaction) equation in a continuum[14]. In this context, a significant contribution on the effect of diffusion in the presence of reaction is made by Sokolov and Blumen,[15−19] who analyze the statistical and scaling properties of lamellar systems in one- and two-dimensional model structures. These structures are designed to represent the state of a mechanically premixed system at a time when the convective mixing has stopped, and reaction and molecular diffusion are started (e.g., by suddenly increasing the temperature of the system). Attention should also be drawn to the approach based on lobe-dynamics proposed in ref 20, which essentially involves application of the Melnikov theorem to characterize transport in weakly perturbed integrable Hamiltonian flows.[21]

The strong impulse given by recent attempts toward the understanding of mixing processes from a global geometric standpoint suggests that the interplay between diffusion and

* Author to whom correspondence should be addressed. E-mail: max@giona.ing.uniroma1.it.

10.1021/jp004290h CCC: $20.00
Published on Web 05/01/2001

advection could be approached in a slightly different perspective, namely by determining how the invariant properties characterizing the geometry of chaotic flows are modified by diffusion, and consequently to what extent the theoretical results derived on partially mixed structures in the absence of diffusion can be applied to understand and predict the outcome of real mixing processes. Remarkably enough, this point has been object of intense discussion within the *fast dynamo* community, where the physical background of the mathematical analysis is to determine the conditions in which a magnetic field seed stirred by a forcing convective flow can exhibit overall exponential growth.[22−24]

In this article we try to approach this issue, without claiming to offer a solution, by specifically focusing on phenomenological features and orienting the analysis in a global geometric perspective. In this respect, classical scaling laws on the temporal behavior of the mean square displacement are of little use, and attention is instead focused on the time evolution of material interfaces subjected to diffusion. To achieve a quantitative description of the phenomena, two basic quantities are introduced, namely diffusional thickness, and area of diffusional influence (see section 3 for a definition). The temporal behavior of these quantities is analyzed by means of numerical simulations on a model two-dimensional closed chaotic flow. This analysis makes it possible to identify the global effect of diffusion on the spatial configuration of partially mixed structures. More specifically, it is possible to define a characteristic time-scale, τ_D, up to which it is still reasonable to envision mixing as a convective process of ever thickening interfaces. At times shorter than τ_D, the concentration fields of the components being mixed therefore appear as blurred images of the interface distribution corresponding to the purely advective limit. At times larger than τ_D, the striations begin to merge with one other, and the geometric structure inherited from the convective template is irreversibly destroyed. From the scaling of the diffusional thickness and the area of influence, it is also possible to define an effective interface length, which provides an overall measure of the combined action of convection and diffusion.

As mentioned above, this article is essentially descriptive, and its basic goal is to propose a new method of approaching real mixing processes in closed chaotic flows. The remainder is organized as follows. Section 2 provides a succinct description of the invariant geometry of partially mixed structures in two-dimensional time-periodic chaotic flows. Section 3 defines the basic quantities related to the geometrical characterization of the interplay between diffusion and advection as regards interface evolution. Section 4 analyzes the numerical results obtained for a model flow system that possesses all the qualitative features of two-dimensional periodically forced viscous flows. Section 5 briefly addresses how this approach can help toward an understanding of chemical reactions in these systems, at least in qualitative terms.

2. Global Geometry of Partially Mixed Structures

Many physicochemical phenomena that evolve in a fluid system subjected to mixing are significantly controlled by the geometry of interfacial structures. For example, a chemical reaction between initially segregated species occurs as the species diffuse into and encounter one another in a "reaction zone" located around the interface (in the limit of an infinitely fast reaction, this zone collapses onto the interface itself). This process is clearly enhanced by the increase in interface length. Loosely speaking, optimal yield and control conditions for a reacting flow are associated with convective fields that can distribute the interface densely through nearly all of the flow domain while stretching it exponentially. The term "partially mixed structures" generically indicates both the geometry of closed interfaces and the spatial configuration of fluid elements surrounded by these interfaces.

In the presence of nonlinear kinetics and/or spatially varying flow fields, it is intuitively clear that a description of the system based on a single overall parameter such as global interface growth is likely to be insufficient, and the fine spatial details of the interface distribution need to be taken into account.

As mentioned in the Introduction, passive interface dynamics has recently been the object of intense investigation. This section provides only a brief summary of the main results of these studies. Those interested in the details are referred to the cited literature.[7−9,21,25]

Consider a two-dimensional closed flow system generated by a periodically forced velocity field that is chaotic on a given subregion C of the flow domain (hereafter referred to as the main chaotic region). As the flow is time-periodic, the kinematics can be studied in a stroboscopic time frame where snapshots of the system are taken at multiple integers of the period, say T_p. The time-discrete analogous of eq 1 is thus

$$\mathbf{x}_{n+1} = \Phi(\mathbf{x}_n) \tag{2}$$

where the mapping Φ (Poincarè map) yields the new position $\mathbf{x}_{n+1}$ of a point located at $\mathbf{x}_n$ after a time T_p.

Within the main chaotic region C, let us now consider the evolution of an interface γ (closed curve, boundary of a fluid element) sampled at the period of the forcing term. The sequence of curves $\gamma_n = \Phi^n(\gamma)$ for large n tends to fill C and to display invariant patterns in their geometric structure. More specifically, for sufficiently large n, the tangent vector to γ_n at a point $x \in \gamma_n$ is oriented in the direction of the unstable invariant subspace at that point, $\epsilon^u_{\mathbf{x}}$. This implies that the set of all the one-dimensional unstable invariant subspaces $\{\epsilon^u_{\mathbf{x}}\}_{\mathbf{x}\in C}$, referred to as the unstable sub-bundle, is the intrinsic geometric template that characterizes the asymptotic invariant geometry of partially mixed structures.

To give an example, which will be used throughout the article, let us consider a model flow on the two-dimensional torus, i.e., sine flow,[26] the velocity field of which is given by

$$\mathbf{v} = (v_x, v_y)^T$$

where

$$\begin{array}{lll} v_x = v_o \sin(2\pi y), & v_y = 0, & 2nT \le t < (2n+1)T \\ v_x = 0, & v_y = v_o \sin(2\pi x), & (2n+1)T \le t < (2n+2)T \end{array} \tag{3}$$

where $T_p = 2T$ is the period, $n = 0, 1, \ldots$, and v_o is a constant. With no loss of generality we may assume $v_o = 1$ au. The Poincarè map associated with the time-periodic velocity field eq 3 can be expressed in closed form and is given by

$$\Phi(x) = \begin{cases} x + T\sin(2\pi y) & \text{mod. } 1 \\ y + T\sin[2\pi(x + T\sin(2\pi y))] & \text{mod. } 1 \end{cases} \tag{4}$$

Although sine flow is a highly idealized model, it is able to capture the qualitative properties of physically realizable periodically forced two-dimensional chaotic flows, and can be used as a prototype of these systems for theoretical and numerical investigation.

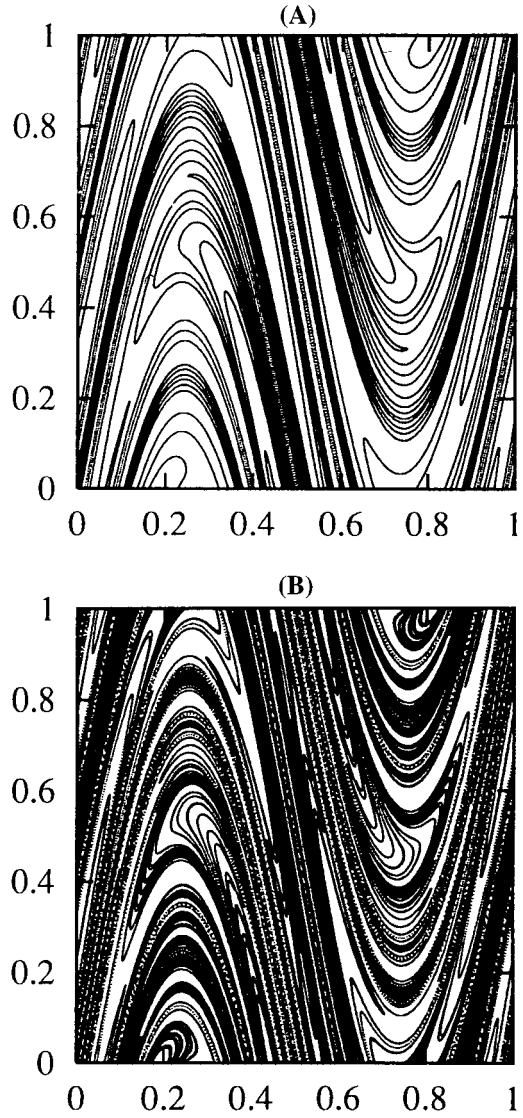

Figure 1. Evolution of a material interface $\gamma_o = \{x = 1/2 \quad 0 \le y \le 1\}$ for the sine flow map eq 4 at $T = 0.8$. (A) $n = 2$, (B) $n = 3$.

Figure 1 shows the evolution of a curve γ for $T = 0.8$ at times $n = 2, 3$. The most striking feature is the geometric invariance that characterizes the evolution of partially mixed structures. This geometric invariance can be quantitatively described by means of intermaterial interface density, as developed elsewhere.[8,9] Together with the scaling behavior of interface length with time,[27,28] it constitutes the basic information on the global evolution properties of partially mixed structure in pure advection.

3. Characterization of Interface Evolution in the Presence of Diffusion

From the discussion developed in section 2, it follows that the salient features of the interplay between advection and diffusion are mainly related to the modification of the geometric properties of partially mixed structures. Scaling analysis of mean square displacement in aperiodic flows is of little use in this connection. In particular, very little information is provided about partially mixed structures by analysis of the mean square displacement of fluid particles in chaotic flows on the torus (such as sine flow, or the ABC flow considered by Jones[11]), in which the periodicity conditions of the mixing space (corresponding to the compact topology of the torus) are relaxed and particle motion is considered on an infinite Euclidean space (often used to characterize diffusional effects in chaotic flows).

To account for the diffusional modifications induced on interface dynamics, a natural starting point is to analyze the spatiotemporal evolution of an interfacial mass discontinuity, i.e., to consider a closed compact set I embedded in the flow domain and track the evolution of the concentration field starting from an initial condition where one of the species is concentrated on the boundary ∂I. In a continuum formulation, this leads to the partial differential equation

$$\frac{\partial \psi}{\partial t} + \mathbf{v}\cdot\nabla\psi = \frac{1}{Pe}\nabla^2\psi \tag{5}$$

equipped with the initial condition

$$\psi(\mathbf{x}, t = 0) = A\delta_{\gamma_o}(\mathbf{x}) \tag{6}$$

where $\delta\gamma_o(\mathbf{x})$ is an impulsive (Dirac's delta) function along the initial interface (which is a closed surface), and A is a normalization constant that makes the integral of the initial condition over the whole mixing space (in this case the two-dimensional torus) equal to unity. In eq 5 $Pe = vL/D$ is the Peclet number, i.e., the ratio of the characteristic diffusion time to the characteristic convection time, where v, L, and D are, respectively, the reference velocity, length, and diffusivity of the system. All the quantities in eq 5 are dimensionless. The velocity field entering into eq 5 is given by eq 3, and the only parameter characterizing advection is the half period T.

Equations 5 and 6 correspond to the propagation of an initial concentration discontinuity centered at the interface of separation of two fluid elements. To give an example related to the toral geometry of the mixing space characterizing sine flow, if the two fluid species are initially segregated and placed, respectively, in the left and right vertical portions ($0 < x < 1/2$ and $1/2 < x < 1$), the initial interface consists of two circumferences located respectively at $x = 0$ and $x = 1/2$, and the initial condition is given by

$$\psi(\mathbf{x}, t = 0) = \frac{\delta(x) + \delta(x - (1/2))}{2} \tag{7}$$

With some precautionary steps, eq 5 can be solved numerically. It is advisable to make use of a finite-volume formulation in place of finite-difference schemes, as the latter can, if used without due caution, produce numerical inconsistencies, such as local negative values of the discretized concentration field ψ. It is important to stress that eq 5 does not represent the evolution of the intermaterial interface density (the equation for which encompasses the effects of the deformation tensor in the stretching of a material interface) but is the mass balance equation associated with an initial interfacial discontinuity corresponding to the initial segregation of the two fluid species.

The first problem to be solved is how to extract from eq 5 the relevant information about the implication of a diffusive term in the evolution of partially mixed structures.

It is a fairly obvious step to approach interfacial dispersion by considering the concentration isograms of the field ψ. Initially the field ψ is localized with an impulsive profile at the interface γ_o. The evolution of $\psi(\mathbf{x}, t)$ produces a progressive dispersion and, at $t \to \infty$, $\psi(\mathbf{x}, t) = \psi_\infty = 1$, uniformly all over the mixing space. To quantify the diffusive propagation, it is possible to consider the graph of the level curves $\psi(\mathbf{x}, t) = \psi_r$, where ψ_r is a constant reference value. The choice of ψ_r is arbitrary in some respects. Its value should be chosen close to unity in order to enhance the effect of diffusion but, as will be shown in the

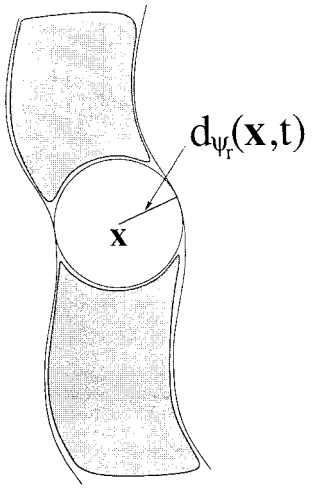

Figure 2. Schematic representation of the geometrical meaning of the diffusional thickness $d_{\psi r}(\mathbf{x}, t)$.

next section, its value is not particularly important for the early stages of the process, which are in any case those of greatest significance. Two different values of ψ_r were chosen, namely $\psi_r = 0.9$ and $\psi_r = 1$, to show that the quantitative description of the mixing process is weakly sensitive to the choice of ψ_r.

The isogram approach to dispersion leads to the following definition of the domain of diffusional influence:

$$D_{\psi r}(t) = \{\mathbf{x} | \psi(\mathbf{x}, t) > \psi_r\} \tag{8}$$

i.e., $D_{\psi r}(t)$ is the set of points at which the concentration field is higher than the reference value ψ_r. It follows from this definition that a measure of the spatial extent of the diffusional propagation is given by the normalized area of diffusional influence $\phi_{\psi r}(t)$ defined as

$$\phi_{\psi r}(t) = \frac{\mathrm{mis}(D_{\psi r}(t))}{\mathrm{mis}(M)} \tag{9}$$

where mis(A) indicates the measure (or area in a two-dimensional system) of the set A, and M is the mixing region (in our case the two-dimensional torus). Of course, if $\psi_r < 1$ then $\lim_{t\to\infty} \phi_{\psi r}(t) = 1$.

The analysis of diffusion obtained by considering $\phi_{\psi r}(t)$ should be complemented by other information describing the evolution in time of a characteristic thickness of the lamellar structure associated with the spatial configuration of the domain of diffusional influence $D_{\psi r}(t)$. This can be achieved as follows. Let $\mathbf{x}$ be a point belonging to $D_{\psi r}(t)$, and let $B(\mathbf{x}, \epsilon)$ be a ball of diameter ϵ centered at $\mathbf{x}$. The local diffusional thickness $d_{\psi r}(\mathbf{x}, t)$ at point $\mathbf{x}$ can be defined as the diameter of the largest ball centered at $\mathbf{x}$ and contained within $D_{\psi r}(t)$, i.e., $B(\mathbf{x}, d_{\psi r}(\mathbf{x}, t)) \subseteq D_{\psi r}(t)$. Figure 2 shows a schematic picture of the geometrical meaning of $d_{\psi r}(\mathbf{x}, t)$. The average of this quantity over $D_{\psi r}(t)$ yields the diffusional thickness $d_{\psi r}(t)$ at time t:

$$d_{\psi r}(t) = \frac{1}{\mathrm{mis}(D_{\psi r}(t))} \int_{D\psi r(t)} d_{\psi r}(\mathbf{x}, t)\, d\mathbf{x} \tag{10}$$

In numerical simulations, this definition should be slightly modified in order to account for the discretized description of the mixing space, and to make its evaluation computationally efficient. The local diffusion thickness at a lattice site $\mathbf{x_i}$ can be defined a the minimum value between the diameters in the two coordinate directions x and y passing through $\mathbf{x_i}$ and fully contained within the region of diffusional influence.

4. Numerical Results

Two values of the parameter T entering into eq 4 are considered, namely $T = 0.4, 0.8$. For $T = 0.8$ the main region of chaotic behavior of eq 1 extends over nearly the whole torus, while for $T = 0.4$ islands of quasiperiodic motion are clearly detectable. These landscapes of the mixing space represent the two basic phenomenologies encountered in the kinematics of passive tracers advected by chaotic flows. Peclet values range in the interval $200 \div 5000$, and the size of the discretized lattice utilized to solve eq 5 ranges from 400×400 to 1600×1600 (the higher the Peclet number, the larger the lattice needed in order to obtain accurate numerical results).

Figure 3 shows the evolution of the domain of diffusional influence $D_{\psi r}(t)$ for $\psi_r = 0.9$ at the early stage of the process (i.e., up to the first three-half periods) for $Pe = 1000$, starting from the initial condition eq 7 corresponding to the interface discontinuity between two fluid species distributed symmetrically around $x = 1/2$. The solid lines show the advection of the initial interface.

As can be observed, up to time $t = 0.9$ (Figure 3 a−c)), the interfacial discontinuity progressively broadens while retaining its characteristic geometrical form as a "fattened" curve. The domain $D_{0.9}(t)$ resembles a "sausage" elongated in space and centered about the advected initial interface. In this situation, the diffusional thickness $d_{\psi r}(t)$ defines an average measure of the broadening of the original interface. Up to this time, diffusion makes no qualitative change to the lamellar configuration of partially mixed structures. At time $t = 1.0$ (Figure 3 d) a drastic change in the structure of $D_{0.9}(t)$ occurs. Two lamellae centered in different portions of the advected interface are brought by advection up to a diffusional lengthscale and merging occurs. We refer to this phenomenon as lamellae breakdown or merging, and to the first time instant at which it occurs as the merging time τ_D.

The picturresque terminology in the preceeding paragraph is neither new nor original, being borrowed from the physical description of chaotic attractors for dissipative sustems in the presence of noise ("fat fractals"). Similarly, the description of the structure of $D_{\psi r}$(t) as a "sausage" derives from the box-counting methods (the Minkowski sausage) applied to fractal sets and interfaces.

Surprisingly, lamellar breakdown takes place in the very early stages of the mixing process, even at comparatively high Peclet numbers ($\sim$1000−5000). For example, at $Pe = 1000$ and $T = 0.8$, τ_D is of the order of the first half period of motion.

The merging time is a significant factor for the fate of partially mixed structures. As can be observed from Figure 3 e,f, the structure of $D_{0.9}(t)$ starts to deviate from the broadening of the convective interfacial backbone slightly after τ_D. This deviation becomes significant after one period of motion, at which time the interfacial convective backbone and the domain of diffusional influence already look altogether different.

It might be supposed that diffusional effects will eventually come to dominate after the first merging of neighboring lamellae, and the area of diffusional influence will invade the entire mixing space. This is not what happens, as can be observed in Figure 3 g,h). The structure of $D_{0.9}(t)$ rearranges itself after the initial period to recreate a simple lamellar structure that continues to be convected, stretched along the unstable directions, and expanded in space due to diffusion in a nonmonotonic way until perfectly mixed conditions are achieved.

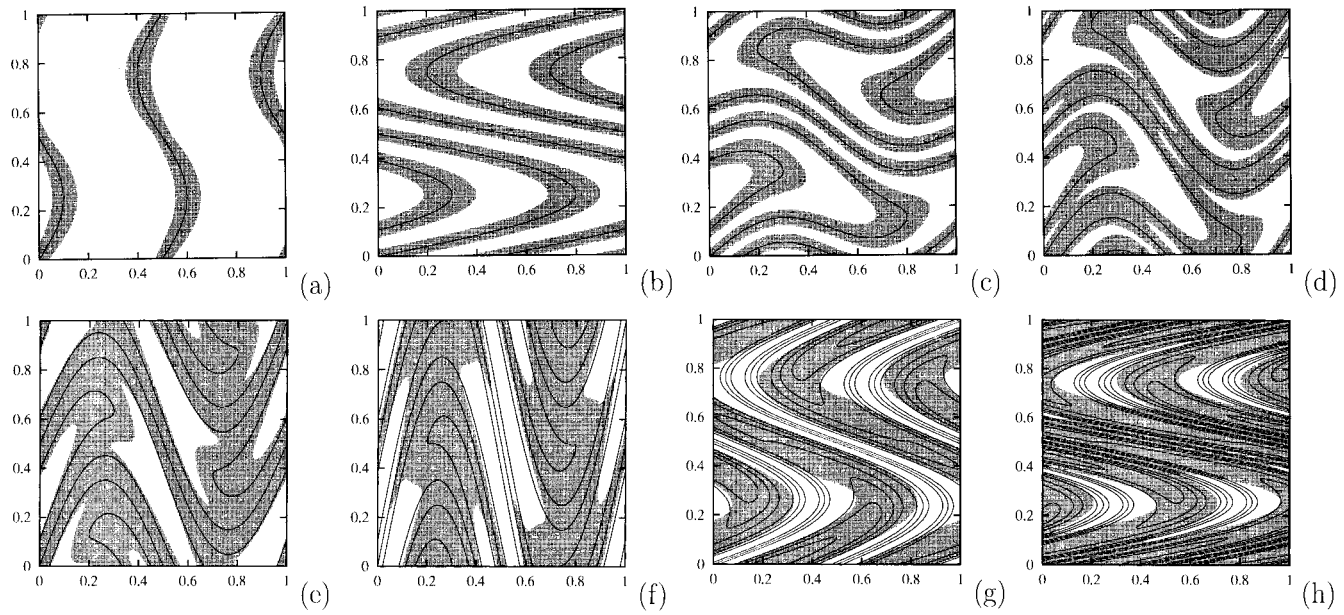

Figure 3. Spatial structure of the domain of diffusional influence $D_{0.9}(t)$ (dotted region) obtained by solving eq 5 starting from the initial condition (7) for $T = 0.8$ and $Pe = 1000$. (a) $t = 0.1$,(b) $t = 0.8$, (c) $t = 0.9$, (d) $t = 1.0$, (e) $t = 1.2$, (f) $t = 1.6$, (g) $t = 2.0$, (h) $t = 2.4$. Solid lines are the evolutions of the initial interface (circumferences at constant x located at $x = 0$ and $x = 1/2$) in the absence of diffusion.

This qualitative description indicates that the evolution of partially mixed structures under the influence of diffusion follows a nearly periodic process in which periodicity is a consequence of diffusional merging of lamellae followed by reorientation of the newborn lamella along the local unstable invariant directions. The result of these processes is a nonmonotonic propagation of the diffusion front, the quantitative properties of which are discussed below.

Let us first consider the behavior of the diffusional thickness in the early stages of the process. Figure 4 A,B shows the behavior of $d_{0.9}(t)$ for sine flow at $T = 0.8$ (Figure 4 A) and during the first half period of motion (Figure 4 B). The latter figure shows a nonmonotonic behavior of the diffusional thickness, which displays a local maximum independently of the Peclet number.

This phenomenon is a consequence of the interplay between the diffusional broadening and the shrinking of the lamellar structure along the stable directions. A simple dynamic model for $d_{\psi r}(t)$ can be expressed as follows:

$$\frac{\mathrm{d}d_{\psi r}(t)}{\mathrm{d}t} = \frac{\mathrm{d}\sigma(t)}{\mathrm{d}t} - \lambda_s d_{\psi r}(t) \tag{11}$$

where

$$\sigma(t) = \left(\frac{4t}{Pe}\right)^{1/2} \tag{12}$$

The first term on the right-hand side of eq 11 expresses the rate of diffusional propagation, which is inversely proportional to the Peclet number and to the square root of time. The second term in eq 11 corresponds to the exponential shrinking along the stable directions. Equations 11and 12 can be integrated to yield

$$d_{\psi r}(t) = \frac{2}{Pe^{1/2}} \mathrm{e}^{-\lambda_s t} \int_0^t \mathrm{e}^{\lambda_s y^2} \mathrm{d}y \tag{13}$$

Equations 11 and 12 remain valid until different lamellae interact with one other, i.e., up to time-scales of the order of the merging time τ_D. Equation 13 yields a nonmonotonic behavior of $d_{\psi r}(t)$,

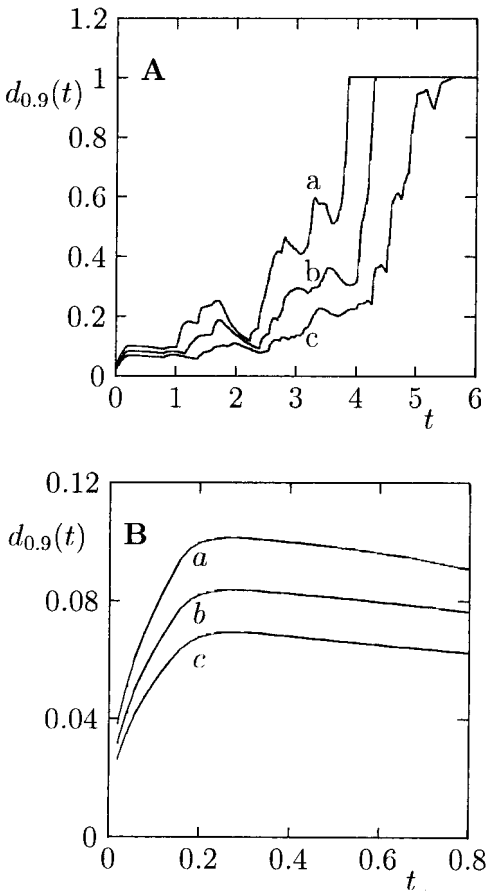

Figure 4. (A) $d_{0.9}(t)$ vs t at $T = 0.8$. (a) $Pe = 1000$, (b) $Pe = 2000$, (c) $Pe = 5000$. (B) Snapshot of the first half period of motion. (a) $Pe = 1000$, (b) $Pe = 2000$, (c) $Pe = 5000$.

which possesses a local maximum at a time instant τ_m independently of the value of the Peclet number. This behavior is confirmed by numerical simulations (see Figure 4 B), which yield for τ_m the values $\tau_m = 0.26$ for $T = 0.8$ and $\tau_m = 0.27$ for $T = 0.4$ (the values of the exponent λ_s are equal to 3.0 and 2.8, respectively, in the two cases).

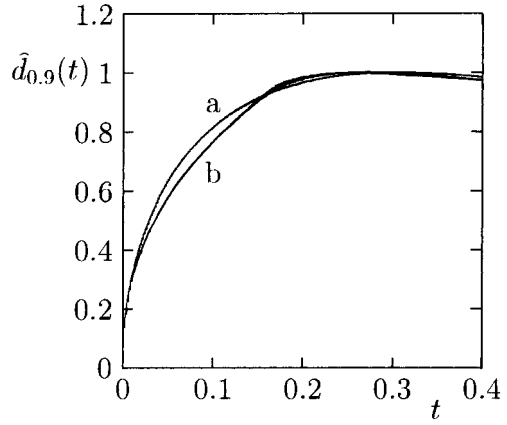

Figure 5. Normalized diffusional thickness $\hat{d}_{0.9}(t)$ vs t at $T = 0.4$. Curve (a) is the theoretical prediction eq 13, curves (b) are the simulation results for $Pe = 1000$, 2000, 5000 collapsing into a single curve.

The validity of the model can be checked from its qualitative predictions. From eq 13 it follows in fact that the normalized diffusional thickness $\hat{d}_{\psi r}(t)$, obtained by rescaling $d_{\psi r}(t)$ with respect to the value attained at the local maximum, is independent of the value of Pe. This means that $\hat{d}_{\psi r}(t)$ is a master curve onto which the numerical results obtained at different values of the Peclet number should collapse. Figure 5 compares the simulation results and eq 13 is depicted, showing $\hat{d}_{0.9}(t)$ for $T = 0.4$. This figure indicates a satisfactory level of agreement between model predictions and simulations. The result is also satisfactory in view of the fact that the process of shrinking along the unstable directions is highly nonuniform in space, and that the shrinking rate varies from point to point. It should also be observed that the exponent λ_s is not an intrinsic asymptotic property of the system, since the behavior shown in Figure 5 occurs in the very early stages of the mixing process and may in principle depend on the location of the initial interface.

Let us now consider the behavior of the area of diffusional influence. Figure 6 A,B shows the behavior of $\phi_{0.9}(t)$ and $\phi_{1.0}(t)$ vs time for different values of the Peclet number. In the early stages of mixing, i.e., up to $t \simeq 2.4$, the influence of the threshold ψ_r is practically negligible. For longer times, $\phi_{0.9}(t)$ saturates toward unity while $\phi_{1.0}(t)$ attains small values, as expected, and its dynamics is characterized by an oscillating behavior. The different behavior of $\phi_{0.9}(t)$ and $\phi_{1.0}(t)$ is important for a qualitative understanding of the mixing process. The time instant at which $\phi_{0.9}(t)$ saturates toward unity is a parameter related to the time-scales at which the concentration field reaches an almost uniform distribution over the whole mixing space. This occurs at $t \simeq 3.8$ for $Pe = 1000$ and $t \simeq 5.5$ for $Pe = 5000$ ($T = 0.8$). The nonmonotonic behavior observed for $\phi_{0.9}(t)$ below $t = 2.4$, and the oscillation characterizing the evolution of $\phi_{1.0}(t)$ are a manifestation of contraction effects along the stable subbundle in opposition to the irreversible diffusional broadening.

These oscillatory effects in diffusional propagation are the most characteristic feature of chaotic flows. It is important to stress that these phenomena are clearly detectable (and to the best of our knowledge observed and discussed for the first time in connection with laminar chaotic flows) by means of the descriptive apparatus proposed in this article, but much more difficulty to capture through standard statistical approaches.

Quantitative support of this latter observation is provided by considering the mean square displacement $\sigma^2(t) = \langle(\mathbf{x}(t) - \langle\mathbf{x}(t)\rangle)^2\rangle$ of an ensemble of passive particles (in the simulations the number of particles is order 5×10^5) initially located at a point $\mathbf{x}_o$. Being of absolutely no importance as regards the results

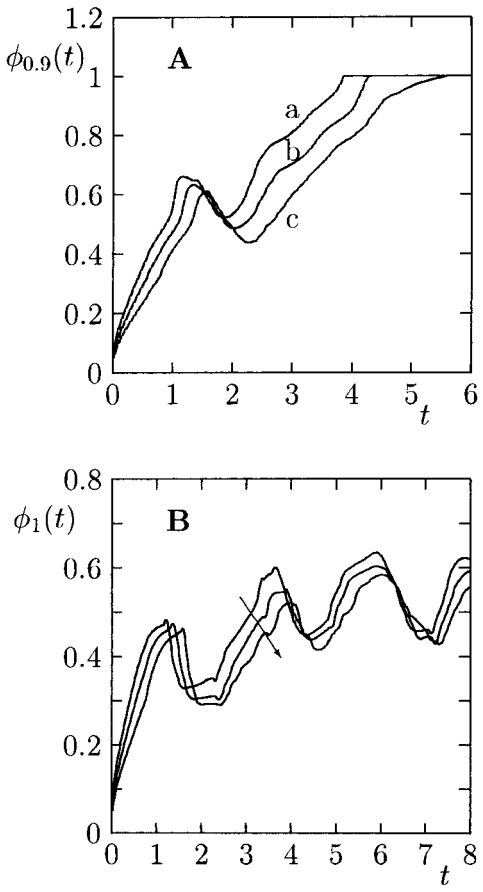

Figure 6. (A) $\phi_{0.9}(t)$ vs t at $T = 0.8$. (a) $Pe = 1000$, (b) $Pe = 2000$, (c) $Pe = 5000$. (B) $\phi_{1.0}(t)$ vs t at $T = 1.0$. The arrow indicates increasing values of the Peclet number, $Pe = 1000$, 2000, 5000.

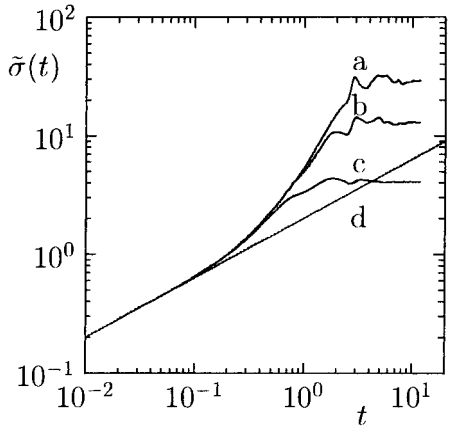

Figure 7. $\tilde{\sigma}(t) = \sigma(t)Pe^{1/2}$ vs t at $T = 0.8$. (a) $Pe = 5000$, (b) $Pe = 2000$, (c) $Pe = 1000$. Line (d) is $\tilde{\sigma}(t) = (4t)^{1/2}$.

of the present analysis, the initial point was set at $\mathbf{x}_o = (1/2, 1/2)$. Figure 7 shows the behavior of $\tilde{\sigma}(t) = \sigma(t)Pe^{1/2}$ at $T = 0.8$ for several values of the Peclet number. At short time scales, $\tilde{\sigma}(t)$ follows the scaling $\tilde{\sigma}(t) = (4t)^{1/2}$ (line d) in Figure 7), and afterward increases in almost monotonic fashion toward saturation. The small amplitude oscillations that can be observed close to saturation are in fact indicative of the nonmonotonic evolution of the area of diffusional influence, but it is more difficult to infer geometric properties of partially mixed structures from these results than from those relative to $\phi_{\psi r}(t)$ or $d_{\psi r}(t)$.

Another interesting piece of information that can be obtained through the approach discussed in section 3 follows from another simple geometric observation. Let us again consider Figure 3a,b.

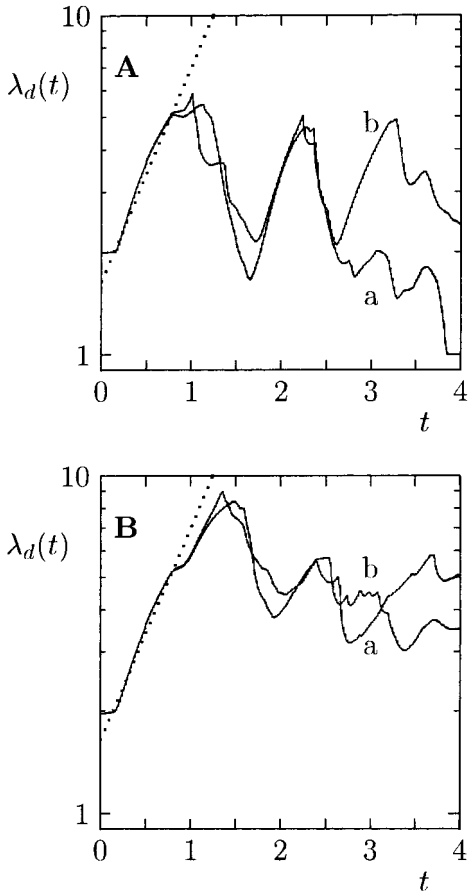

Figure 8. $\lambda_d(t)$ vs t at $T = 0.8$. (A) $Pe = 1000$, (B) $Pe = 5000$. Curves (a) refer to the threshold $\psi_r = 0.9$, curves (b) to $\psi_r = 1.0$. The dotted line is the scaling $\lambda_d(t) \sim \exp(\theta t/2T)$, with $\theta = 2.33$.

For $t < \tau_D$, the area of diffusional influence is organized around a convective backbone given by the advected interface corresponding to the initial discontinuity. It is a natural step to define an effective interfacial length $\lambda_d(t)$ as the ratio between the area of diffusional influence and the diffusional thickness,

$$\lambda_d(t) = \frac{\phi_{\psi r}(t)}{d_{\psi r}(t)} \tag{14}$$

$\lambda_d(t)$ will of course depend on the choice of the threshold value ψr. Equation 14 can be viewed as a consequence of the fact that the area of diffusional influence is centered around the curvilinear backbone given by the advected initial interface, with an average width equal to the diffusional thickness. Figure 8A,B shows the behavior of $\lambda_d(t)$ for two values of the Peclet number corresponding to the threshold values $\psi_r = 0.9$ and $\psi_r = 1.0$. The dotted line is the scaling of the length of a material interface (in the absence of diffusion)

$$\lambda_d(t) \sim \exp\left(\frac{\theta t}{2T}\right) \tag{15}$$

where the exponent θ, known as *topological entropy*,[29,30] is strictly greater than the Liapunov exponent of the system.

For $T = 0.8$, $\theta = 2.33 \pm 0.02$. Figure 8 indicates that for $t < \tau_D$ ($\tau_D \simeq 1.0$ for $Pe = 1000$, $\tau_D = 1.35$ for $Pe = 5000$), $\lambda_d(t)$ follows the convective scaling eq 15, and possesses its absolute maximum in the neighborhood of τ_D $\lambda_d(t)$.

This leads to an alternative definition of the merging time as the time instant at which $\lambda_d(t)$ reaches its maximum value. Comparison of the behavior of $\lambda_d(t)$ for the two values of the threshold considered indicates that the choice of the threshold has no effect on the results up to $t \simeq 2.5$. This provides further support for the view that the results obtained are essentially an intrinsic feature of the mixing process and do not depend on the choice of ψ_r.

The maximum value of $\lambda_d(t)$ attained ranges from $\lambda_d \simeq 6$ for $Pe = 1000$, up to $\lambda_d = 9.3$ for $Pe = 5000$, thus indicating that the maximum interfacial elongation attained in a diffusion-convection process is rather low as a result of the merging kinetics of neighboring lamellae.

The fact that the quantity $\lambda_d(t)$ compares so well with the stretching of an advected line in the early stage of the mixing process bears out the idea that within this time frame the combined action of chaotic advection and diffusion can be spatially decoupled into two different processes, namely exponential stretching along the local unstable directions (expressed by $\lambda_d(t)$) and diffusional growth along the orthogonal direction (expressed by $d_{\psi r}(t)$, thus confirming the physical meaning of the quantities introduced.

5. Some Observations on Chemical Reactions

The qualitative and quantitative description of diffusion/convection kinetics emerging from the approach developed in this article can be used to achieve a better understanding of other physicochemical processes evolving in mixing systems.

This section briefly considers the case of chemical reactions. The aim is not to provide a thorough analysis of the complex dynamics of reaction/diffusion kinetics in laminar chaotic flows, but rather to outline how the description of mixing in the presence of diffusion developed in sections 3 and 4 may be helpful in situations that depart from a purely diffusive/convective setting.

Let us consider an elementary bimolecular kinetics A + B → Product in a chaotic flow. The balance equations in dimensionless form read as follows:

$$\frac{\partial c_A}{\partial t} = -\mathbf{v}\cdot\nabla c_A + \frac{1}{Pe}\nabla^2 c_A - \frac{\phi^2}{Pe} c_A c_B$$

$$\frac{\partial c_B}{\partial t} = -\mathbf{v}\cdot\nabla c_B + \frac{1}{Pe}\nabla^2 c_B - \frac{\phi^2}{Pe} c_A c_B \tag{16}$$

where c_A and c_B are the concentrations of the two reactants, ϕ is the Thiele modulus, $\phi^2 = k c_r L^2/D$, where k is the kinetic rate coefficient for the second-order reaction, c_r is a reference concentration, L a characteristic lengthscale of the system, and D the diffusivity. The reactants are initially segregated: $c_A(\mathbf{x}, t = 0) = 1$ for $0 \le x < 1/2$, $0 \le y < 1$, while opposite relationships hold for the other reactant, $c_B(\mathbf{x}, t = 0) = 1$ for $1/2 \le x < 1$, $0 \le y < 1$. This configuration corresponds to the interfacial discontinuity eq 7 analyzed in sections 3 and 4. In the simulation of eq 16 use was made of a finite-volume algorithm. This is more robust that finite difference schemes in that it prevents the occurrence of negative concentration values.

The major practical difficulty in approaching eq 16 is that, despite the formal simplicity of the problem, very large lattices are needed in order to obtain reliable numerical results.[31,32] Moreover, the lattice size increases dramatically with the Peclet number. To give an example, Figure 9 A) shows the time behavior of the reactant concentration $C_A(t) = \int c_A(\mathbf{x}, t) d\mathbf{x}$ at $Pe = 1000$ and $\phi^2/Pe = 10$ (corresponding to a fast reaction), for different lattice sizes $N \times N$, starting from $N = 100$ to $N = 800$ (from the overall mass balance it directly follows that $C_A(t) = C_B(t)$). For this value of the Peclet number, reproducible

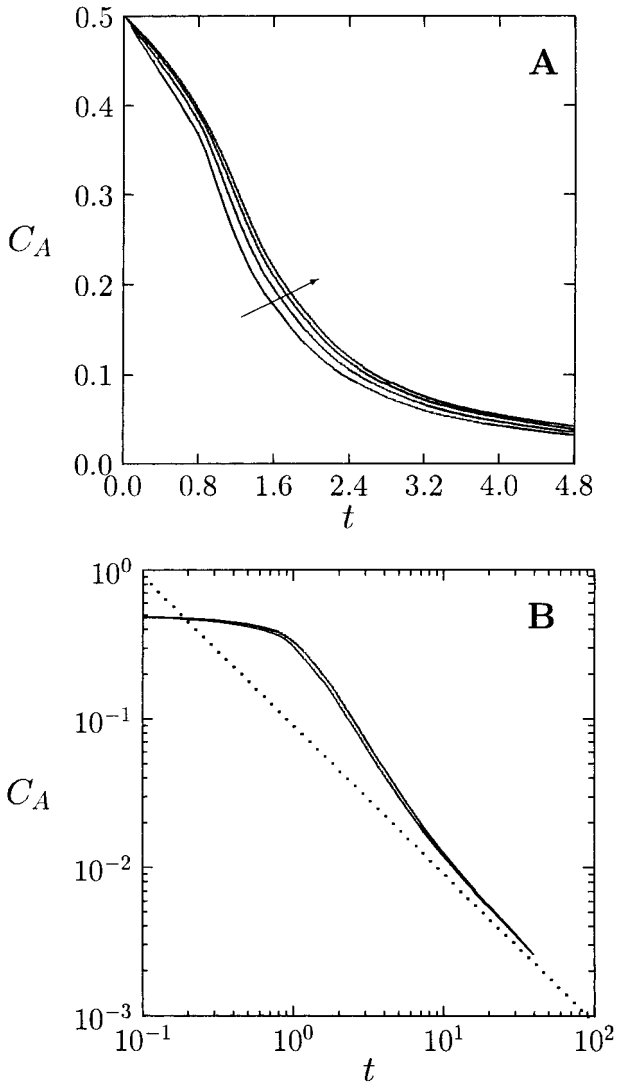

Figure 9. $C_A(t)$ vs t for $Pe = 1000$. (A) The arrow indicates increasing values of the lattice size $N \times N$, $N = 100, 200, 400, 800$. (B) log−log plot of $C_A(t)$ vs t. The dotted lines is the scaling laws $C_A \sim t^{-1}$.

and size-independent data are obtained for a 800 × 800 lattice (numerical results obtained for a 1200 × 1200 lattice are nearly indistinguishable from those corresponding to a 800 × 800 lattice). For $Pe = 5000$, the lattice size required is of the order of magnitude of 5000 × 5000. This phenomenon has been attributed to the creation of a complex lamellar structure formed by regions in which one of the reactants is almost exclusively present. The numerical results obtained in section 4 for convection/diffusion processes suggest that this hypothesis does not agree with the system evolution. Even at comparatively high Peclet numbers, reaction−diffusion kinetics is not controlled by the formation of hundreds of striations but rather by the occurrence of sharp discontinuities in the concentration fields of the two reactants that develop in a much simpler lamellar structure composed of about 10 striations (even at $Pe = 5000$). This observation comes from analysis of the temporal behavior of effective interfacial length $\lambda_d(t)$. Since the dimensionless characteristic length of the system is 1, the value of $\lambda_d(t)$ can be roughly regarded as a measure of the total number of lamellae in the mixing system.

This observation is further supported by a simple scaling observation on the evolution of the reactant quantity $C_A(t)$. Figure 9B shows the log−log plot of $C_A(t)$ vs t for the data of Figure 9B. Starting from $t \simeq 4-5$, the conversion time curve sets to the scaling $C_A(t) \sim t^{-1}$ (dotted line) corresponding to almost perfectly mixed conditions of the two reactants, and the crossover time is of the same order of magnitude as the time instant at which $\phi_{0.9}(t)$ saturates.

This result indicates that all the complex features of a reaction−diffusion kinetics in chaotic flows occur at relatively short time scales and involve only a few lamellae. The numerical difficulties in simulating the evolution of reactive processes should be therefore attributed to the space resolution in the simulation of sharp discontinuities, which can be tackled by means of specific numerical tools able to capture these features at reasonable computer costs in terms of both CPU time and memory requirements. To this end, wavelet collocations in the form proposed by Vasilyev and Paolucci[33,34] appear to be a promising alternative to more classical numerical methods based on finite differences or finite volumes. The analysis of fast reaction kinetics in chaotic flows further indicates that the characterization of partially mixed structures based on the area of diffusional influence provides a measure for the time scales at which almost perfectly mixed conditions are attained.

6. Concluding Remarks

This article develops a simple but physically significant approach to the analysis of geometrical properties of partially mixed structures under diffusion in two-dimensional chaotic flows. In the early stages of the mixing process, the two quantities introduced, namely effective interfacial length λ_d and diffusional thickness $d_{\psi r}$ make it possible to envisage the intertwined actions of diffusion and convection quantitatively as two spatially independent processes, i.e., a convective stretching of the diffusional area in the local unstable direction and a diffusional broadening in the orthogonal direction.

Extension to three-dimensional system is a straightforward matter, as the approach is not grounded on any specific property of two-dimensional structures.

Although the approach is grounded on an arbitrary choice of the threshold level ψ_r, the results prove to be substantially independent of this choice, at least for the early time-scales at which most of the salient features occur.

Diffusional propagation in laminar chaotic flows is characterized by a nonmonotonic behavior resulting from the competition between diffusional propagation, which tends to invade the mixing space, and shrinking along the stable direction induced by the chaotic nature of the kinematics. This phenomenon can be clearly detected from the analysis of diffusional thickness at short time scales before merging, the behavior of which can be predicted correctly by a simple model, eq 11, taking into account these two effects.

Another significant result stemming from this analysis is that diffusion prevents the formation of a two-complex lamellar structure, even for comparatively high values of the Peclet number ∼5000). The effective interfacial length $\lambda_d(t)$ barely reaches the value of 10 at $Pe = 2000-5000$, and this indicates that the complex features observed in the dynamics of reaction/diffusion kinetics cannot be attributed to the formation of a lamellar structure composed of hundreds or thousands of striations, but rather to the occurrence of sharp discontinuities in the mixing space at the interface between very few (usually less than 10) lamellae.

The quantitative information on spatial structure and time scales that can be obtained by the analysis, say, of the temporal behavior of the area of diffusional influence in order to predict the attainment of almost perfectly mixed conditions within the

system is in agreement with the scaling analysis of reaction−diffusion kinetics in these systems.

References and Notes

(1) Ottino, J. M. *The kinematics of mixing: stretching, chaos and transport*; Cambridge University Press: Cambridge, 1989.
(2) Ottino, J. M. *Chem. Eng. Sci.* **1980**, *35*, 1377.
(3) Chella, R.; Ottino, J. M. *Chem. Eng. Sci.* **1984**, *39*, 551.
(4) Fields, S. D.; Ottino, J. M. *Chem. Eng. Sci.* **1987**, *42*, 459.
(5) Aref, H. *J. Fluid Mech.* **1984**, *143*, 1.
(6) Middleman, S. *Fundamentals of polymer processing*; McGraw-Hill: New York, 1977.
(7) Alvarez, M. M.; Muzzio F. J.; Cerbelli, S.; Adrover, A.; Giona, M. *Phys. Rev. Lett.* **1998**, *81*, 3395.
(8) Giona, M.; Adrover, A. *Phys. Rev. Lett.* **1998**, *81*, 3864.
(9) Giona, M.; Adrover, A.; Muzzio, F. J.; Cerbelli, S.; Alvarez, M. M. *Physica D* **1999**, *132*, 298.
(10) Aref, H.; Jones, S. W. *Phys. Fluids A* **1989**, *1*, 470.
(11) Jones, S. W. *Phys. Fluids A* **1991**, *3*, 1081.
(12) Jones, S. W. *Chaos, Solitons Fractals* **1994**, *4*, 929.
(13) Glück, M.; Kolevsky, A. R.; Korsch, H. J. *Physica D* **1998**, *116*, 283.
(14) Dopazo, C.; Calvo, P.; Petriz, F. *Phys. Fluids* **1999**, *11*, 2952.
(15) Sokolov, I. M.; Blumen, A. *Phys. Rev. A* **1991**, *43*, 6545.
(16) Sokolov, I. M.; Blumen, A. *Int. J. Mod. Phys. B* **1991**, *5*, 3127.
(17) Sokolov, I. M.; Blumen, A. *Phys. Rev. A* **1991**, *43*, 2714.
(18) Sokolov, I. M.; Blumen, A. *Physica A* **1992**, *191*, 177.
(19) Reigada, R.; Sagues, F.; Sokolov, I. M.; Sancho, J. M.; Blumen, A. *Phys. Rev. Lett.* **1997**, *78*, 741.
(20) Rom-Kedar, V.; Poje, A. C. *Phys. Fluids* **1999**, *11*, 2044.
(21) Beigie, D.; Leonard, A.; Wiggins, S. *Chaos, Solitons Fractals* **1994**, *4*, 749.
(22) Du, Y.; Ott, E. *J. Fluid. Mech.* **1993**, *257*, 265.
(23) Du, Y.; Ott, E. *Physica D* **1993**, *67*, 387.
(24) Klapper, I. *Phys. Fluids A*, **1992**, *4*, 861.
(25) Poje, A. C.; Haller, G.; Mezic, I. *Phys. Fluids* **1999**, *11*, 2963.
(26) Liu, M.; Muzzio, F. J.; Peskin, R. L. *Chaos, Solitons Fractals* **1994**, *4*, 869.
(27) Beigie, D.; Leonard, A.; Wiggins, S. *Phys. Rev. Lett.* **1993**, *70*, 275.
(28) Adrover, A.; Giona, M.; Muzzio, F. J.; Cerbelli, S.; Alvarez M. M. *Phys. Rev E* **1998**, *58*, 1.
(29) Block, L.; Keesling, J.: Li, S.; Peterson, K. *J. Stat. Phys.* **1989**, *55*, 929.
(30) Newhouse, S.; Pignataro, T. *J. Stat. Phys.* **1993**, *72*, 1331.
(31) Muzzio, F. J.; Liu, M. *Chem. Eng. J.* **1996**, *64*, 117.
(32) Zalc, J. M.; Muzzio, F. J. *Chem. Eng. Sci.* **1999**, *54*, 1053.
(33) Vasilyev, O. V.; Paolucci, S.; Sen, M. *J. Comput. Phys.* **1995**, *120*, 33.
(34) Vasilyev, O. V.; Paolucci, S. *J. Comput. Phys.* **1996**, *125*, 498.